The Synchrotron Shock Model Confronts a "Line of Death" in the BATSE Gamma-Ray Burst Data

R. D. Preece, M. S. Briggs, R. S. Mallozzi, G. N. Pendleton, and W. S. Paciesas
Dept. of Physics, University of Alabama in Huntsville, Huntsville, AL 35899
and

D. L. Band
Center for Astrophysics and Space Sciences, Code 0424,
University of California at San Diego, La Jolla, CA 92093

ABSTRACT

The synchrotron shock model (SSM) for gamma-ray burst emission makes a testable prediction: that the observed low-energy power-law photon number spectral index cannot exceed $-2/3$ (where the photon model is defined with a positive index: $dN/dE \propto E^{\alpha}$). We have collected time-resolved spectral fit parameters for over 100 bright bursts observed by the Burst And Transient Source Experiment on board the *Compton Gamma Ray Observatory*. Using this database, we find 23 bursts in which the spectral index limit of the SSM is violated. We discuss elements of the analysis methodology that affect the robustness of this result, as well as some of the escape hatches left for the SSM by theory.

Subject headings: gamma rays: bursts — radiation mechanisms: non-thermal

1. Introduction

Gamma-ray bursts (GRBs) have been an astronomical puzzle for 30 years. Details of the gamma-ray emission from bursts are still elusive, although there is an emerging agreement that persistent afterglow emission at other wavelengths from locations consistent with those of several recent GRBs can be related to expanding fireballs at cosmological distances (Goodman 1986, Metzger et al. 1997, Waxman 1997). One promising mechanism that has been proposed for gamma-ray emission is the synchrotron shock model (SSM): synchrotron emission from particles accelerated in a relativistic shock is Lorentz-boosted into the gamma-ray band (Rees & Mészáros 1992, Mészáros & Rees 1993, Rees & Mészáros 1994, Katz 1994a, Tavani 1996). The SSM identifies the spectral break observed in most burst spectra with the characteristic synchrotron energy in the emitter's rest frame, boosted into the observer's frame. Thus, the fitted energy of the spectral break would contain information about both the bulk Lorentz motion of the emitters and the equipartition magnetic field producing the synchrotron radiation (Tavani 1995). In addition, the SSM makes the specific prediction that the low-energy power-law spectral index of the observed photon number spectra should not exceed $-2/3$, with the assumption that the optical depth of the shocked material is less than unity. We use the convention that the power-law index α takes a positive sign: $dN/dE \propto E^{\alpha}$. The $-2/3$ value is derived from the synchrotron single-particle emission spectrum: bulk relativistic motion ensures that the mean particle energy is large enough that there are few low-energy particles (Katz 1994a, Tavani 1995). Below the cyclotron fundamental energy, the low-energy spectrum is approximately that produced by mono-energetic particles and is thus independent of their actual distribution and should be a constant $-2/3$ spectral index power law. If that were the total story, the model would already be rejected, since it is well-known that bursts are observed to have a variety of spectral behaviors at low energies (Band et al. 1993, Preece et al. 1996, Strohmayer et al. 1997, Crider et al. 1997). However, it also has been noted that the timescale for synchrotron cooling of the particles may be shorter than the duration of burst pulses (Katz 1994b, Sari, Narayan & Piran 1996, Sari & Piran 1997). A cooling distribution of particles is characterized by a power-law index of -2, which translates into a $-3/2$ photon number index through the synchrotron power-law emission formula (Rybicki & Lightman 1979). If one includes the effects of cooling of the particle distribution, the low-energy spectral index can encompass the range of $-3/2$ to $-2/3$. However, the spectral slope still cannot be greater than the fundamental single-particle limit of $-2/3$.

In this *Letter*, we test the SSM limit on spectral behavior by examining how well the data support it. We draw our results from a catalog of time-sequences of spectral fits to 137 bursts selected for their high flux and fluence, using (mostly) Large-Area Detector (LAD) data from the Burst And Transient Source Experiment (BATSE) on the *Compton Gamma Ray Observatory* (see Preece et al. 1998 for details of the analysis). In the next section, we determine the best spectral indicators derivable from the data and show how they should bracket the 'true' low-energy spectral behavior. In §3, for each of the bursts in the catalog we compare the effective low-energy power-law spectral index with the SSM limit line. Finally, in §4 we discuss the implications these results have on further theoretical modeling.

2. Spectral Modeling

The model typically chosen for spectral fitting of bursts is the empirical 'GRB' function (Band et al. 1993):

$$\begin{aligned} f(E) &= A(E/100)^{\alpha}\exp\left[\frac{-E(2+\alpha)}{E_{\rm peak}}\right] \\ \text{if} \quad E &< \frac{(\alpha-\beta)E_{\rm peak}}{(2+\alpha)} \equiv E_{\rm break}, \qquad (1) \\ \text{and} \quad f(E) &= A\left[\frac{(\alpha-\beta)E_{\rm peak}}{100(2+\alpha)}\right]^{(\alpha-\beta)}\cdot \\ & \qquad \exp{(\beta-\alpha)(E/100)^{\beta}} \\ \text{if} \quad E &\geq \frac{(\alpha-\beta)E_{\rm peak}}{(2+\alpha)}, \end{aligned}$$

where the four model parameters are: the amplitude A, a low-energy spectral index α, a high-energy spectral index β and an energy $E_{\rm peak}$ that corresponds to the peak of the spectrum in $\nu\mathcal{F}_{\nu}$ if β is less than -2. In this expression, $E_{\rm peak}$ and α are jointly determined by the low-energy continuum, while β is solely determined by the spectrum above the break energy, $E_{\rm break}$. If this break energy lies above the highest energy available to the detector, β is ill-defined, so we must substitute a related form of the model with the high-energy power-law omitted. In cases where

a sharp inherent curvature of the spectrum results in an unacceptable value of χ^2 for a fit to the GRB spectral form, a broken power-law (BPL) model often generates better results.

Observed burst spectra are such that the data rarely approach the GRB spectral low-energy power-law within the energy range of BATSE and most other burst experiments. At the low end of the spectrum, α is approached only asymptotically, as seen by comparing the dotted line in Figure 1 with the GRB model fit to an example spectrum (*solid line*). The model-dependent photon 'data' rates consist of photon model rates weighted by the ratios of the deconvolved model rates and the count rates in each data channel, allowing different photon models to be represented simply on a single plot. A better measure of the actual lower-energy behavior is an effective spectral index, e. g., the slope of the power-law tangent to the GRB function at some chosen energy ($E_{\rm fid}$), which can be found analytically:

$$\left.\frac{d\ln f(E)}{d\ln E}\right|_{E_{\rm fid}} \equiv \alpha_{\rm eff}(E_{\rm fid}) = \alpha - (2+\alpha)\frac{E_{\rm fid}}{E_{\rm peak}}. \quad (2)$$

For typical values of α, i. e., $\alpha > -2$, $\alpha_{\rm eff}(E_{\rm fid})$ will always be less than α by an amount that depends upon the value chosen for $E_{\rm fid}$. We chose $E_{\rm fid} = 25$ keV for the following reasons: The observed spectrum is consistent with the GRB function above about 25 keV; below this value, deviations from the standard GRB function have been observed that may indicate the existence of an additional low-energy spectral component (Preece et al. 1996). In addition, 25 keV is just greater than the low-energy cut-off for the LADs; it is above an electronic spectral distortion in the SDs at typical gain settings (Band et al. 1992) and it is also below fitted values for $E_{\rm peak}$ in nearly all bursts. The effective spectral index at 25 keV will be denoted α_{25}. Once $E_{\rm fid}$ has been fixed, the correction gets smaller as the fitted value for $E_{\rm peak}$ gets larger, since $\alpha_{\rm eff}$ is closer to the asymptotic value α. This is also seen in Figure 1, where $E_{\rm peak} = 1308$ keV, so $\alpha = -0.04 \approx \alpha_{25}$ (the GRB function is not appropriate for this spectrum and is shown for illustration only). In any practical case, α_{25} serves as an upper bound on the low-energy spectral index, in the sense that it is more positive than an average slope through the model. We will use α_{25} in this work, rather than α, since it is more indicative of the slope actually seen in the data.

To the extent that all burst spectra have continuous curvature rather than a sharp break, a BPL function fit (Figure 1 – *dashed line*) will generate a spectral index (which we will call $\alpha_{\rm PL}$) that is a lower bound on the 'true' low-energy spectral behavior, in that it will be more negative than it would be for a model that takes into account some curvature, such as the GRB function. Thus, to be conservative in our estimate for how well the BATSE data support the SSM, $\alpha_{\rm PL}$ provides the best available comparison, since if it lies above the limiting $-2/3$ line, we can be reasonably sure the 'true' spectrum will violate the SSM. Of course, this will do us no good if the BPL model is not an acceptable fit to the data. Thus, we use fits to two models to put bounds on the 'true' low-energy spectral behavior: α is a model parameter asymptotic to the data, but we can approximate the upper bound with the quantity α_{25} defined above. The BPL estimate, $\alpha_{\rm PL}$, is a lower bound.

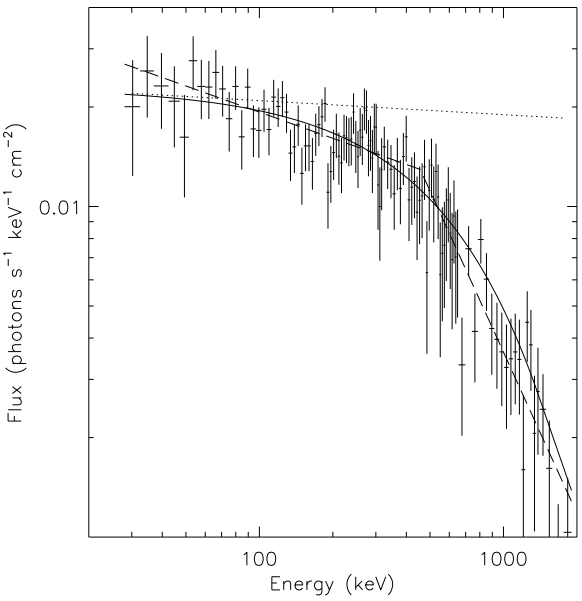

Fig. 1.— Photon spectrum accumulated between 0.448 – 0.768 s after the trigger for 3B910814. Two best-fit models are plotted on top of the deconvolved data: the GRB function (*solid line*) and the BPL model (*dashed line*; $\alpha_{\rm PL} = -0.263$). The tangent slope at 25 keV is also shown: $\alpha = -0.04$ (*dotted line*). Neither model is as steep as $-2/3$ at low energies. The errors represent model variances.

3. Observations

In Figure 2, we show results from our BATSE catalog of time-resolved spectroscopy of bright bursts (peak flux > 10 ph cm^{-2} s^{-1} and fluence $> 4 \times 10^{-5}$ erg cm^{-2}), using mostly LAD data. The value of α_{25} is plotted against $E_{\rm peak}$ for the spectrum in each burst for which α_{25} reaches its maximum value. In addition to the α_{25} – $E_{\rm peak}$ parameters obtained by fitting the GRB function, we have also included $\alpha_{\rm PL}$ – $E_{\rm break}$ pairs (*diamonds*) for those bursts where use of the BPL model was more appropriate. Overlaying this plot is the synchrotron $-2/3$ spectral index 'death line' (*dashes*), as well as the lower bound allowed for cooling distributions (*dotted line*). The SSM is quite safe within these boundaries; however, 44% of the total have maximum low-energy spectral indices above $-2/3$, in a region that is totally excluded in the SSM. In particular, 32% of the BPL bursts have points that lie above this line. With some correlation between the two displayed parameters, the most stringent limits are set by the spectral indices of spectra with the highest values of $E_{\rm peak}$, as well as any bursts that have a BPL index greater than $-2/3$. Clearly, many such bursts exist; one is the example shown in Figure 1, which is a BPL fit with $\alpha_{\rm PL} = -0.263$ and $E_{\rm break} = 456$ keV, the highest-energy diamond above the $-2/3$ limiting line.

The error bars shown in Figure 2 represent the 1σ error for each parameter considered singly, as obtained from the covariance matrix of the fit. If the errors in the determination of the spectral index were not normally distributed, perhaps having a broad tail instead, then values that are much greater than the SSM limit of $-2/3$ might violate the SSM. To test this, we created 4 sets each of 1000 simulated spectra, based on the GRB model spectrum propagated through the detector response, with random Poisson fluctuations determined for the counts in each data channel. These consisted of bright, medium and dim spectra, with expected errors of 0.06, 0.2 and 0.34, respectively, for the fitted value of α. The parameter values assumed were $\rm E_{break} \sim 400$ keV, $\beta = -2$ and $\alpha = -2/3$, to provide a worst case test. A second set of medium-brightness spectra was also created, to test the effect of a small assumed value of $\rm E_{break} = 200$ keV. A histogram of the resulting fitted α values is approximately consistent with a Gaussian distribution for each set, however, distributions for the dimmer sets of spectra have slightly extended tails on the

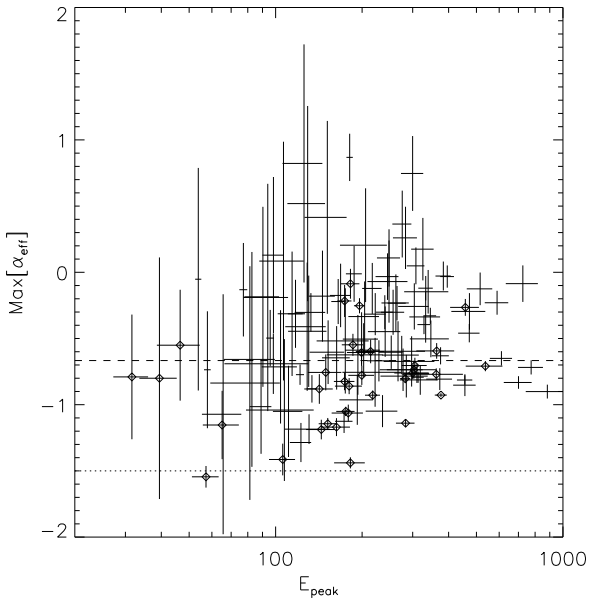

Fig. 2.— A plot of fitted low-energy power-law index against $E_{\rm peak}$. The spectrum chosen for each burst is the one with the largest value of α. Diamonds indicate bursts fit with a broken power-law model. The SSM-violating region is bounded from below by the 'death line' (*dashed*) and the acceptable region is bounded by the $-3/2$ line (*dotted*). Points where the error bars on α_{25} exceed the plot area were omitted for clarity.

side of more positive values of α. These larger values all have large computed errors associated with them, so the resulting distributions of deviations of α from the mean, weighted by their errors (see below), do not have a tail. Rather, the average over the 4 simulations for the number of error-weighted deviations greater than 2 σ is 7.25, compared with the 22.7 deviations expected for 1000 trials in a normal distribution. Interestingly, the effect where large values of α have larger associated errors can be observed in Figure 2, where the errors above the $-2/3$ line are, on average, 1.5 times those below. The KS probability we calculate from comparing the $\alpha > -2/3$ tails between our observations and the simulations is 3×10^{-38} ($D_{\rm KS} = 0.26$ for $N_{\rm obs} = 1012$ and $N_{\rm sim} = 1689$), indicating that it is quite unlikely that the two distributions are the same.

Another way to view these results is as a histogram of $\Delta\alpha_\sigma \equiv (\alpha - (-2/3))/\sigma_\alpha$ (here, we use α to stand

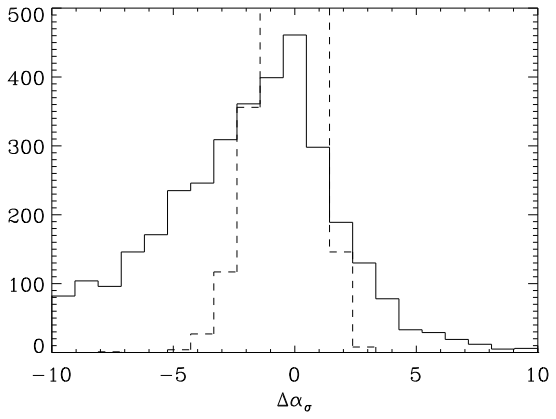

Fig. 3.— A histogram of deviations of the low-energy power-law indices from $-2/3$ in units of their 1σ error for 3957 fitted spectra. Positive deviations represent a violation of the SSM. Also plotted is the distribution of 1σ deviations from the mean for spectra indices obtained from fits to 4000 simulated spectra (*dotted*). The peak has been clipped so that the wings of the two distributions can be compared.

in as a generic low-energy power-law index); that is, the deviation of α from $-2/3$ in units of the standard error for each fit. Figure 3 shows the distribution of $\Delta\alpha_\sigma$ for the entire ensemble of 3957 spectra from the 137 bursts fit, where the SSM-violating region consists of the positive values to the right of zero. There are 312 spectra total in the bins containing 3σ and greater (that is: $> 2.4\sigma$). This may be compared with our expected error distribution, based upon the 4000 total simulated spectral fits described above (Fig. 3 – *dashed line*), where the total over the same bins is 8 (in fact, $0 > 3.4\sigma$). We may estimate the probability that 312 out of 3957 spectra would arise from 2.4σ fluctuations larger than $-2/3$, assuming the SSM prediction that no such spectra exist. The simulations show that the chance probability of a $-2/3$ slope spectra having a fit value more than $+2.4\sigma$ away from $-2/3$ is $\sim 8/4000$. Using the binomial probability distribution, the chance that the observed 312 out of 3957 could result from random fluctuations is $< 10^{-366}$, showing the observations to be quite inconsistent with the SSM.

4. Discussion

We have shown that there are a large number of bursts that violate the limit on low-energy spectral behavior imposed by the basic synchrotron emission mechanism acting in a relativistic shock. It is worthwhile considering which spectral models can accommodate this observation. First of all, it has been suggested (Liang et al. 1997) that Compton upscattering of soft photons by an energetic distribution of particles can significantly modify the basic synchrotron emission spectrum, with energetic particles boosting their own synchrotron emission into the observed gamma-ray band. The details of the spectral shape thus depend upon the particle distribution, as well as the shape of the photon spectrum at the energies where it is being sampled for upscattering. The observed steep low-energy spectral indices would arise for certain combinations of the source parameters and then would evolve to smaller values as the particles cool. An important prediction from this model is that a low-energy component, independent of the observed gamma-ray emission, must be present with sufficient strength to serve as a pool of photons for upscattering. It is indeed possible that this separate component may already have been observed (Preece et al. 1996, Strohmayer et al. 1997). If the low-energy portion is truly an independent component, it will have an independent time history as well. The troubling part of this idea is that *all* bursts should have this component to some extent, since there is no evident bi-modality to the low-energy behavior (cf. Figure 2) that would indicate that the SSM-violating bursts are somehow different.

Synchrotron self-absorption (SSA) is another mechanism that would tend to increase the low-energy continuum spectral index. The maximum photon spectral index that could be observed is $+3/2$, so all of the bursts presented here would be consistent. The photon opacity must be close to unity in all these sources for some to be self-absorbed. For SSA to work the optical depth must be greater than one at energies below $E_{\rm peak}$. Thus, we trade one mystery for another: the narrow distribution of $E_{\rm peak}$ arises in the fact that many bursts have optical depths close to unity, rather than from a narrow distribution of Lorentz factors (see next paragraph). Also, if the photon density is high, it may be very difficult to overcome the opacity arising from photon-photon pair-production.

Since the observed value of $E_{\rm peak}$ should scale as

the bulk Lorentz factor of the emitting material to the fourth power, a narrow observed distribution of $E_{\rm peak}$ implies either that the rest-frame value is extraordinarily precisely determined for all bursts or that the Lorentz factors of the entire ensemble lie in a very narrow distribution. Since neither alternative is satisfactory, Brainerd (1994) proposed that the observed spectra may arise from much different spectra that have been attenuated by intervening material through relativistic Compton scattering. The low-energy behavior is directly related to conditions at the source, namely the optical depth of the scatterers. Large optical depths will result in steep fitted low-energy power-law indices, and the distribution of these should somehow relate to the distribution of densities of the material surrounding putative sources.

Thanks to B. Schaefer who suggested adding error bars to the $\alpha - E_{\rm peak}$ figure from Preece et al. 1996. The anonymous referee has contributed suggestions that have lead to an improved error analysis.

REFERENCES

Band, D. L., et al. 1992, Exp. Astron., 2, 307

Band, D. L., et al. 1993, ApJ, 413, 281

Brainerd, J. J. 1994, ApJ, 428, 21

Cohen, E., Katz, J. I., Piran, T., Sari, R., Preece, R. D., & Band, D. L. 1997, ApJ, 488, 330

Crider, A., et al. 1997, ApJ, 497, L39

Goodman, J. 1986, ApJ, 308, L47

Katz, J. I. 1994a, ApJ, 432, L107

Katz, J. I. 1994b, ApJ, 422, 248

Liang, E. P., Kunose, M., Smith, I. A., & Crider, A. 1997, ApJ, 497, L35

Meegan, C. A., et al. 1996, ApJS, 106, 65 (BATSE 3B Catalog)

Metzger et al. 1997, Nature, 387, 878

Mészáros, P. & Rees, M. J. 1993, ApJ, 405, 278

Preece, R. D., et al. 1996, ApJ, 473, 310

Preece, R. D., et al. 1998, ApJ, 496, 849

Rees, M. J., & Mészáros, P. 1992, MNRAS, 258, 41

Rees, M. J., & Mészáros, P. 1994, ApJ, 430, L93

Rybicki, G. B., & Lightman, A. P. 1979, Radiative Processes in Astrophysics, New York: Wiley, 221

Sari, R., Narayan, R., & Piran, T. 1996, ApJ, 473, 204

Sari, R., & Piran, T. 1997, MNRAS, 287, 110

Strohmayer, T. E., Fenimore, E. E., Murakami, T., & Yoshida, A. 1998, ApJ, 500, 873

Tavani, M. 1995, Ap&SS, 231(1), 181

Tavani, M. 1996, ApJ, 466, 768

Waxman, E. 1997, ApJ, 491, L19

This 2-column preprint was prepared with the AAS LaTeX macros v4.0.